Sensing cell metabolism by time-resolved autofluorescence

Yicong Wu, Wei Zheng, and Jianan Y. Qu

Department of Electronic and Computer Engineering, Hong Kong University of Science and Technology, Clear Water Bay, Kowloon, Hong Kong, China

Received June 23, 2006; accepted August 10, 2006;
posted August 23, 2006 (Doc. ID 72140); published October 11, 2006

We built a time-resolved confocal fluorescence spectroscopy system equipped with the multichannel time-correlated single-photon-counting technique. The instrument provides a unique approach to study the fluorescence sensing of cell metabolism via analysis of the wavelength- and time-resolved intracellular autofluorescence. The experiments on monolayered cell cultures show that with UV excitation at 365 nm the time-resolved autofluorescence decays, dominated by free–bound reduced nicotinamide adenine dinucleotide signals, are sensitive indicators for cell metabolism. However, the sensitivity decreases with the increase of excitation wavelength possibly due to the interference from free–bound flavin adenine dinucleotide fluorescence. The results demonstrate that time-resolved autofluorescence can be potentially used as an important contrast mechanism to detect epithelial precancer. © 2006 Optical Society of America

OCIS codes: 300.6500, 170.1530.

Autofluorescence spectroscopy has been widely explored for noninvasive detection of precancerous development in the epithelium where most human cancers originate. The epithelial fluorescence is mainly determined by the emission of intrinsic fluorophores reduced nicotinamide adenine dinucleotide (NADH) and flavin adenine dinucleotide (FAD), the principal electron donor and acceptor in the cellular metabolic process, respectively. NADH and FAD have been used to probe cell activity for many years.[1,2] In particular, the NADH emits strong fluorescence and the ratio of free to enzyme-bound NADH is a good indicator of the cell metabolic state,[3,4] and the free and bound NADH signals can be differentiated by their fluorescence decay.[4] Recently, we demonstrated that the combined depth- and time-resolved fluorescence spectroscopy can resolve the layered structure of epithelial tissue and extract accurate information on NADH and FAD signals from the total fluorescence of the nonkeratinized epithelial layer.[5] In this work, we extend our study to measure the free–bound NADH fluorescence in epithelial cells and demonstrate that time-resolved fluorescence measurement provides an important contrast mechanism for detecting epithelial precancer.

The schematic of the time-resolved confocal fluorescence spectroscopy system is shown in Fig. 1. The setup is based on the configuration of a standard confocal microscope. The excitation source is the second-harmonic generation of a tunable femtosecond Ti:sapphire laser (Mira900-F, Coherent). A water immersion objective lens (40× and NA=1.15) focuses the excitation beam into the cell samples and collects the backscattered autofluorescence signals. A pair of galvomirrors scan the laser beam and create a 150 μm × 150 μm sampling area in the sample. A 200 μm optical fiber is used as a pinhole to collect the confocal fluorescence and conduct the signal to the spectrometer. The detector is a multichannel time-correlated single-photon-counting (TCSPC) module (SPC-730 and PML-16, Becker & Hickl GmbH) with a linear array of 16 photomultiplier tubes (PMTs) that record fluorescence signals in 16 spectral bands from 400 to 600 nm with a 13 nm interval. The instrument responses of all PMT channels have ~180 ps FWHM. There are no significant temporal shifts between the separate channels. The recorded signal is the averaged fluorescence over the sampling area (150 μm × 150 μm) to minimize the heterogeneity of intracellular fluorescence.[6,7] The samples used in this study were the monolayer cultured SiHa and Ect1/E6E7 cells (The American Type Culture Collection) with 90%–100% confluence, in which SiHa cells are well-known ectocervical cancer cells, while Ect1/E6E7 cells were established from normal ectocervical epithelium immortalized by expression of human papillomavirus 16/E6E7.[8] The excitation power on cell samples was controlled below 100 μW, and the accumulation time was set to 30 s to produce high-quality signals at each wavelength band. A dual-exponential function, $A_1 \exp(-t/\tau_1) + A_2 \exp(-t/\tau_2)$, was used in the fitting analysis of time-resolved cell fluorescence measured from each channel based on the iterative nonlinear least-squares deconvolution.

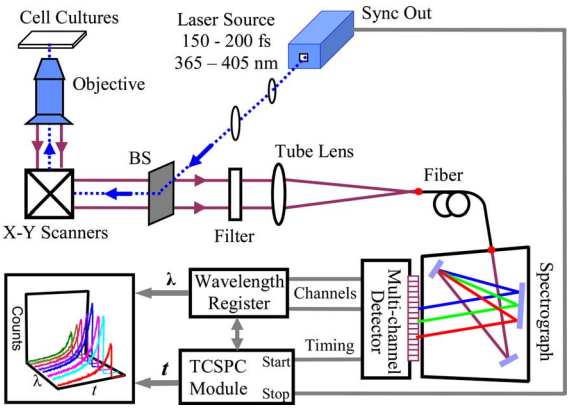

Fig. 1. (Color online) Schematic of the time-resolved confocal fluorescence spectroscopy system.

0146-9592/06/213122-3/$15.00

Our study focused on the spectral and temporal characteristics of the intracellular fluorescence excited at 365 nm, which is dominated by the NADH signal.[3,9] The results of the fitting analysis in three typical wavelength bands and the full band of 16 channels are summarized in Table 1. The fittings were based on the experimental data measured from ten samples. As can be seen, a dual-exponential function provides an excellent description of the intracellular fluorescence decay process, as indicated by the high determination coefficient, r^2. The short and long lifetimes are stable at all emission spectral bands from 400 to 600 nm and comparable with the decay times of free NADH (~0.4 ns) and protein-bound NADH (>1 ns), respectively.[4,10] Moreover, they are consistent with those measured from the nonkeratinized epithelial tissue.[5]

To develop further understanding of the information carried in two lifetime components, we constructed and analyzed the decay-associated spectra (DAS) of short and long lifetime components. In detail, the short and long lifetime DAS were formed with the values of $A_1\tau_1$ and $A_2\tau_2$ calculated from the signals recorded at 16 wavelength bands, respectively. The DAS for the fluorescence signals measured from SiHa and Ect1 samples are shown in Fig. 2. The peaks of short lifetime DAS from SiHa and Ect1 are at ~452 nm. The long lifetime DAS are almost identical and have an ~13 nm blueshift from the short lifetime DAS. It is known that enzyme binding induces the blueshift of NADH fluorescence.[3,11] For comparison, we measured the fluorescence spectra of a pure 500 μM NADH solution (N8129, Sigma-Aldrich) and a 250 μM NADH solution mixed 1:1 with 1000 unit/ml lactate dehydrogenase (LDH, L3916, Sigma-Aldrich), one of several cellular enzymes that can bind with NADH. The results are displayed together with the short and long lifetime DAS of cells in Fig. 2. As can be seen, the LDH binding induces a 13 nm blueshift from the free NADH fluorescence similar to the spectral shifts between long and short lifetime DAS measured from SiHa and Ect1 cell samples. Because free NADH does not contribute to the long lifetime component, the long lifetime DAS should represent the spectra of bound NADH in cells except the possible interference from FAD fluorescence beyond 520 nm.[3,9] Though the short lifetime DAS have the signal peaks and line shapes close to the free NADH signal, the small blueshifts from the free NADH cause little shoulders in the wavelength range from 400 to 450 nm as shown in Fig. 2(a). This indicates some contribution of bound NADH to the short lifetime component because the fluorescence decay of bound NADH is usually multiexponential with short lifetime components comparable with that of free NADH.[12,13] Therefore the short lifetime component could be mainly determined by free NADH with certain interference of bound NADH.

Table 1. Fitting Analysis of Cellular Fluorescence Excited at 365 nm

Cell Line	λ (±5 nm)	τ_1 (ns)	τ_2 (ns)	r^2
SiHa	439 nm	0.42±0.03	3.71±0.17	0.997±0.001
	478 nm	0.43±0.03	3.60±0.28	0.997±0.001
	530 nm	0.41±0.04	3.29±0.25	0.992±0.003
	Full	0.42±0.05	3.59±0.38	0.990±0.012
Ect1	439 nm	0.44±0.01	3.62±0.14	0.997±0.001
	478 nm	0.46±0.02	3.48±0.13	0.998±0.001
	530 nm	0.47±0.03	3.41±0.18	0.995±0.003
	Full	0.45±0.04	3.55±0.30	0.995±0.009

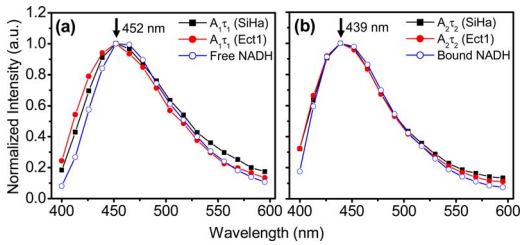

Fig. 2. (Color online) (a) Normalized short lifetime DAS of SiHa and Ect1 cells and the fluorescence spectrum of pure NADH. (b) Normalized long lifetime DAS of SiHa and Ect1 cells and the fluorescence spectrum of LDH-bound NADH.

To investigate the correlation of two lifetime components with the cellular metabolic state, the fluorescence time decay was measured from SiHa and Ect1 samples before and after being treated with the mitochondrial inhibitor sodium cyanide (NaCN) and uncoupler carbonyl cyanide-3-chloro-phenylhydrazene (CCCP).[9] With the excitation at 365 nm, no obvious changes of short and long lifetimes were observed after with NaCN and CCCP. The ratios of the amplitudes of two lifetime components (A_1/A_2) as a function of wavelength band are displayed in Figs. 3(a) and 3(b). As can be seen, the A_1/A_2-ratio values increase with treatment from NaCN and decreased with treatment from CCCP, indicating that the A_1/A_2 ratio is a sensitive indicator for cell metabolism. The result is consistent with the study in other cell samples.[14] In addition, it was found that the A_1/A_2 ratio generally increases with the increase of wavelength (400–530 nm) because of the blueshift of the bound NADH fluorescence with respect to the free NADH fluorescence. Because of the contribution of bound NADH to the short lifetime component in the wavelength range from 400 to 450 nm, the A_1/A_2 ratio measured in the long wavelength region (e.g., 460–600 nm) should produce a more accurate estimation of the free–bound NADH ratio. Furthermore, we compared the A_1/A_2 ratios between SiHa and Ect1 cell samples. The comparison shown in Fig. 3(c) demonstrates that the A_1/A_2 ratios in Ect1 cells are significantly lower than in SiHa cells. The two types of cells established from the same tissue site can be clearly differentiated based on the measurement of time-resolved cellular fluorescence. The higher A_1/A_2 ratios in SiHa cells is in accordance with the findings of Galeotti *et al.* on the loss of binding sites for NADH in malignant cells causing an increase of free NADH concentration.[2] The loss of binding sites for NADH in malignant cells could be related to the anaerobic metabolism in neoplastic cells.[15]

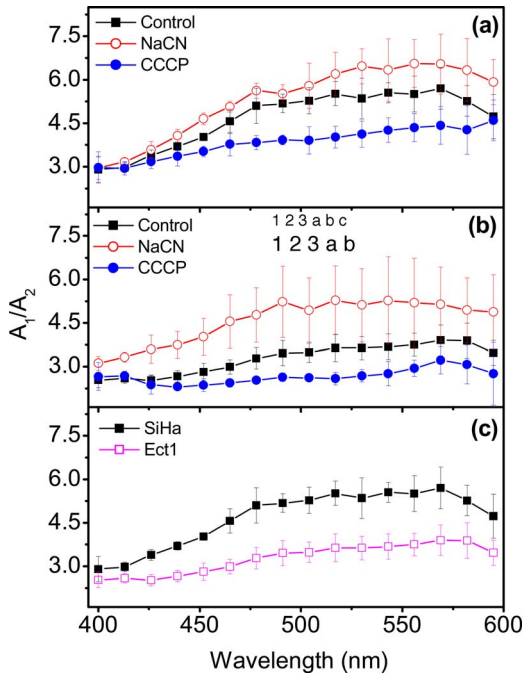

Fig. 3. (Color online) Variation of the A_1/A_2 ratio as a function of wavelength. (a) SiHa cells treated before and after with NaCN and CCCP. (b) Ect1 cells treated before and after with NaCN and CCCP. (c) Comparison between SiHa and Ect1 cells.

Table 2. Analysis of Time-Resolved Fluorescence Measured from SiHa Cells with an Excitation Range from 365 to 405 nm

Excitation		365 nm	385 nm	405 nm
Control	τ_1 (ns)	0.42±0.03	0.38±0.02	0.37±0.03
	τ_2 (ns)	3.60±0.13	3.22±0.10	3.82±0.02
	A_1/A_2	4.02±0.13	3.88±0.18	3.71±0.11
NaCN	A_1/A_2	4.65±0.20	4.26±0.19	3.78±0.15
	Increase	16%	10%	2%
CCCP	A_1/A_2	3.52±0.17	3.53±0.19	3.64±0.15
	Decrease	13%	9%	2%

Finally, we investigated the effect of excitation wavelength on the time-resolved fluorescence sensing of cell metabolism. We tuned the laser wavelength in the range from 365 to 405 nm to excite the fluorescence signals from SiHa samples before and after being treated with NaCN and CCCP. As listed in Table 2, the short lifetime (τ_1) and the long lifetime (τ_2) are different at three typical excitation wavelengths at 365, 385, and 405 nm. More importantly, the NaCN- and CCCP-induced changes of the A_1/A_2 ratio are highly dependent on the excitation wavelength. Here, the fluorescence in the wavelength band from 447 to 457 nm was chosen to calculate the A_1/A_2 ratio because the signal in this band is dominated by NADH signals.[3,5,9] After cells were treated with NaCN and CCCP, the changes of the A_1/A_2 ratio decrease with the increase of excitation wavelength, meaning that the time-resolved fluorescence becomes less sensitive to the cell metabolic activity at long excitation wavelength. In particular, the contrast in the A_1/A_2 ratio before and after treatment with NaCN and CCCP almost disappears at the 405 nm excitation. This may be caused by the increased interference from the FAD fluorescence because FAD and NADH signals reach the balanced level at 405 nm excitation.[5] Though free FAD fluorescence has a long lifetime, the decay of bound FAD fluorescence is multiexponential including a short lifetime component.[10] Therefore FAD fluorescence contributes to both lifetime components and affects the A_1/A_2 ratio.

In conclusion, the decay of cellular fluorescence can be well described by a dual-exponential function. The long lifetime component carries the information of bound NADH, and the short lifetime component is mainly determined by free NADH with certain interference from bound NADH. We demonstrate that the A_1/A_2 ratio can clearly differentiate SiHa cells from Ect1 cells, the cell lines established from cancerous and normal epithelial tissues at the same site, the ectocervix. In future work, we will study the time-resolved fluorescence of neoplastic and normal cell lines and further explore the method to detect neoplastic growth in the epithelium using the combined depth- and time-resolved fluorescence technique.

The authors gratefully acknowledge the support of the Hong Kong Research Grants Council through the grants HKUST6025/02M and HKUST6408/05M. J. Y. Qu's e-mail address is eequ@ust.hk.

References

1. B. Chance, P. Cohen, F. Jobsis, and B. Schoener, Science **137**, 499 (1962).
2. T. Galeotti, G. D. V. VanRossum, D. H. Mayer, and B. Chance, Eur. J. Biochem. **17**, 485 (1970).
3. J. M. Salmon, E. Kohen, P. Viallet, J. G. Hirschberg, A. W. Souter, C. Kohen, and B. Thorell, Photochem. Photobiol. **36**, 585 (1982).
4. A. Pradhan, P. Pal, G. Durocher, L. Villeneuve, A. Balassy, F. Babai, L. Gaboury, and L. Blanchard, J. Photochem. Photobiol., B **31**, 101 (1995).
5. Y. Wu and J. Y. Qu, Opt. Lett. **31**, 1833 (2006).
6. Y. Wu, P. Xi, J. Y. Qu, T. Cheung, and M. Yu, Opt. Express **12**, 3218 (2004).
7. Y. Wu, P. Xi, J. Y. Qu, T. Cheung, and M. Yu, Opt. Express **13**, 382 (2005).
8. R. N. Fichorova, J. G. Rheinwald, and D. J. Anderson, Biol. Reprod. **57**, 847 (1997).
9. N. D. Kirkpatrick, C. Zou, M. A. Brewer, W. R. Brands, R. A. Drezek, and U. Utzinger, Photochem. Photobiol. **81**, 125 (2005).
10. H. Schneckenburger and K. Konig, Opt. Eng. **31**, 1447 (1992).
11. K. Blinova, S. Carroll, S. Bose, A. V. Smironov, J. I. Harvey, J. R. Knutson, and R. S. Balaban, Biochemistry **44**, 2585 (2005).
12. A. Gafni and L. Brand, Biochemistry **15**, 3165 (1976).
13. H. D. Vishwasrao, A. A. Heikal, K. A. Kasischke, and W. W. Webb, J. Biol. Chem. **280**, 25119 (2005).
14. D. K. Bird, L. Yan, K. M. Vrotsos, K. W. Eliceiri, E. M. Vaughan, P. J. Keely, J. G. White, and N. Ramanujam, Cancer Res. **65**, 8766 (2005).
15. A. C. Croce, A. Spano, D. Locatelli, S. Barni, L. Sciola, and G. Bottiroli, Photochem. Photobiol. **69**, 364 (1999).